Oct 18th, 12:00 AM

Finite Element Studies on Lipped Channel Flexural Members

Maria E. Moreyra

Teoman Pekoz

Twelfth International Specialty Conference on Cold-Formed Steel Structures
St. Louis, Missouri, U.S.A., October 18-19, 1994

FINITE ELEMENT STUDIES ON LIPPED CHANNEL FLEXURAL MEMBERS

Maria E. Moreyra[1] and Teoman Peköz[2]

ABSTRACT

This paper is second in a series of three papers describing the research sponsored by the American Iron and Steel Institute. Physical test results described in the first paper combined with the finite element solution parametric studies described in this paper were used in the third paper to develop improved design procedures for edge stiffened elements.

1. INTRODUCTION

Test results [Willis and Wallace (1990a and b)] on lipped channel flexural members have shown some disagreement with the values predicted by the AISI Specification. The main reason for the discrepancies is thought to be the provisions for edge stiffened compression elements. This paper is second in a series of three papers describing the research sponsored at Cornell University by the American Iron and Steel Institute to develop improved design procedures for edge stiffened elements.

The number of parameters determining the strength of lipped channel sections in flexure is large. A physical testing program exploring a wide range of values of these parameters is not practical. For this reason an analytical study using the finite element and finite strip approaches were used to generate a large amount of reliable data to develop a practical design approach.

First the reliability of the finite element approach is established by comparing the computed results with the physical test results. In this determination various parameters for the finite element approach such as convergence criteria, element aspect ratios, stress strain-relationship and initial imperfections are studied.

The computer generated results given in this paper and the physical test results given in the first paper in this series by Moreyra and Peköz (1994a) are used to develop a design approach described in the third paper by Moreyra and Peköz (1994b).

Both the findings of this finite element study and the physical testing agree that an improved design approach for edge stiffened elements is needed.

2. FINITE ELEMENT MODEL

2.1 ABAQUS Program

The program used in this study is ABAQUS. ABAQUS is a finite element analysis program developed by Hibbit, Karlsson & Sorensen (Ref. 1). It is capable of performing geometric and material nonlinear analyses that meet the project needs. Printed and graphical output of stresses and displacements effectively illustrate the analysis results.

In nonlinear problems, a convergent solution must be found in minimum time. ABAQUS automatically controls the time step in all analysis procedures. The user defines certain tolerance or error measures and ABAQUS then automatically increments the load to meet these requirements. This approach is highly effective, especially for buckling problems since response of the model changes drastically in the non-linear range.

---

[1] Engineer, L. E. Robertson Assoc., N. Y., N. Y.

[2] Professor of Structural Engineering, Cornell University, Ithaca, N.Y.

The algorithm chosen for this study is the modified Riks method. This method is effective in obtaining nonlinear static equilibrium solutions for unstable problems. The loading is assumed to be proportional; namely, all load magnitudes vary with a single scalar parameter. The response is assumed to be reasonably smooth without sudden bifurcations.

2.2 CONTROL TEST

Since finite element analyses are sensitive to various input variables (such as material properties, element size, boundary conditions, and initial imperfections), an accurate model must be created before a parametric study can be done. This accuracy was checked by comparing the finite element results to a physical test result which will be referred to as the "control test". The authors used one of their own experiments, test "A-TB" as the control test [Moreyra and Peköz (1994a)].

Experiment "A-TB" consisted of a pair of simply supported 18' lipped channel beams which were laterally braced by steel decks fastened on the top and bottom flange at one foot intervals. Lipped channels were uniformly loaded in a vacuum chamber. The nominal section dimensions (notation for cross-sectional dimensions is shown in Fig. 1) were D = 1 1/8" (28.58 mm), W = 2.5" (63.50 mm), and H = 8.5" (215.90 mm). The thickness was 0.071" (1.80 mm) and the yield stress was 63.5 ksi (437.83 N/mm^2). Details of this experiment can be found in Moreyra and Peköz (1993). The ultimate moment reached by this section was 127.4 k-in (14396.20 N-m).

First an eighteen foot span finite element model was developed. Several mesh configurations were examined and refined. However, due to the time involved in carrying out the analysis, it was decided to use a six foot long, simply supported lipped channel with uniform moment for the parametric analysis. The accuracy of the models examined in this study was verified by comparing the ultimate moments of the control test to the ABAQUS test.

2.3 LOAD AND BOUNDARY CONDITIONS

A finite element model of a beam under constant moment is not simple. Several methods of applying moments were considered and tried. It was found that applying forces at node points that are proportional to the distance from the neutral axis was the simplest and most accurate way of idealizing.

The beam had to be braced laterally to minimize torsional stresses in the section. A two foot brace spacing was sufficient. Braces were represented in the model by restricting motion in the direction normal to the web. This motion was restricted at the center node of both flanges.

The finite element beam has "roller" boundary conditions on all nodes of each end. Restriction of the motion along the member axis is provided at a midspan node. This is necessary for structural stability. All boundary conditions are chosen so that symmetrical stresses develop in the beam and no unusual stress contour patterns develop in these areas.

2.4 MATERIAL PROPERTIES

ABAQUS results indicated that the material stress-strain relationship is a very significant variable for beam behavior and ultimate strength. The material modeled in ABAQUS which most closely resembled the control test material, best matched the control test ultimate moment and stiffness in the elastic and inelastic stage was the tri-linear stress-strain diagram shown in Fig. 1.

2.5 ELEMENT TYPE

ABAQUS has several elements to chose from. The one used in this study is the S9R5 element. It is a nine node shell element with five degrees of freedom.

Shell elements are important for buckling problems because they contain bending degrees of freedom which brick elements do not. This element is sufficiently accurate and efficient for this project's purposes.

2.6 MESH

Since buckling occurs in compression, it is efficient to divide the cross section mesh into tension components and compression components. The parts in compression are divided into more elements than the parts in tension. The number of elements in the corners always remain the same: one element for each corner in tension, and two elements for each corner in compression.

Element displacements along the span, and cross-sectional stresses were plotted for each model at ultimate loads. The conclusions reached on examining the stresses, displacements, and moment at the peak ABAQUS load step are discussed below.

One and two elements were tested in the compression lip. Examination of ultimate moments, displacements and stresses show that the number of elements in the compression lip does not affect the results significantly. One element was used for the compression and the tension lip.

Two and three elements were tested in the compression flange. This variable significantly affects the beam stresses and displacements. Since the ultimate moment reached by the model with three elements in the flange came the closest to the control test ultimate moment, it was assumed that more elements in the compression flange produce a more accurate model. Three elements were used for the compression flange and two for the tension flange.

Two, three, and four elements were modeled in the compression portion of the web. Although the stresses and displacements were not very affected by this variable, the ultimate load results suggest that at least three elements be used in the compression portion of the web. Therefore, three elements were used for the compression portion of the web and two for the tension portion of the web.

Aspect ratios of one, two, and three were studied for the compression elements. Results show that an aspect ratio of three may not be very accurate. There is no difference in results for ratios of one and two. Therefore, a more efficient ratio of two was used for this study.

2.7 INITIAL IMPERFECTION

Three characteristics of the initial imperfection were examined: the imperfection location, magnitude, and shape. The imperfection location was in one of three places: the compression flange only, the web only, or both the web and flange. The model with imperfections in the flange and web have the smallest element displacements. It also is the weakest model of the three.

The size of these imperfections was a multiple of the section thickness, T: 0.5T, 1.0T, and 1.5T. The shape of the imperfections tried along the span was single, two and three half waves along the length of the beam. The smallest imperfection magnitude, 0.5T, produced the greatest displacements and the smallest ultimate moment. The authors think that smaller imperfections allow the beam to displace in its "natural" or dominant form whereas the larger imperfections may change the nature of the displacements in the beam.

The shape in which this imperfection is modeled is very important to the results. The exact control test specimen imperfections are not known. The analysis showed that deformed element wave patterns, or wavelengths, are the same regardless of the imperfection pattern. Therefore, the model with the imperfection pattern that best correlates with the control test ultimate moment will be used. This pattern is three half waves with wavelengths of approximately twenty inches. The model with a triple curvature imperfection

exhibited the greatest element deformations, the greatest stresses, and by far the smallest ultimate load which almost equaled the control test result. The results of the imperfection shape study back up the hypothesis made earlier: imperfections should model the natural deformations.

2.8 ERROR TOLERANCE

ABAQUS (1989) suggests a tolerance of 0.1% to 0.01% of the typical actual force values. The authors defined this force as:

$$P = \frac{(\textit{yield stress})\,(\textit{average compression element length})\,(\textit{thickness})}{6}$$

P is divided by 6 because the S9R5 element distributes the element force along the three side nodes into ratios of 1:4:1. The choice of this parameter affects the quality and efficiency of the nonlinear solution: if the tolerance is too large, the solution will be of poor quality because the equilibrium equation will not be satisfied accurately; if it is too small, excessive iterations will be needed to obtain an acceptable solution which means longer run time.

Three tolerance levels were examined: 0.1%P, 0.05%P, and 0.01%P. The ultimate ABAQUS moment and stresses and displacements at ultimate load showed that there is no difference between the 3 tolerance levels and thus, a tolerance level of 0.1%P was used.

2.9 MODEL CHOSEN FOR PARAMETRIC STUDY

Typical deformed finite element mesh and longitudinal stress contours are shown in Fig. 2. Stresses and displacements in the elastic range are accurate. This may be verified by the reader by comparing the results to those obtained by beam theory. The chosen model has 432 elements and took approximately 8 hours to run on a Vax 4000 work-station.

A typical load versus displacement curve is shown in Fig. 3. The ABAQUS increments are marked on the curve. Stresses at four load points on this graph, A, B, C, and D, are examined on Fig. 4. The "Y-position" on the web and lip, as defined in this figure as well as in other figures, is the vertical distance from the tension flange. Similarly, "Z-position" on the flanges is the horizontal distance from the web. Compression stresses are shown in paranthesis in the horizontal axis. Variation of the stress distribution as the analysis progresses from the elastic range to the post failure range can be seen in Fig. 4. The following observations are made:

- A stress gradient in the compression flange develops in the buckled range. This gradient becomes nonlinear and more pronounced with further increase in load.
- The stresses in the web are linear at least until the ultimate load level. At this point, a significant decrease in stress is observed in the compression portion of the web. This decrease in load suggests that the web may not be fully effective at failure.

The experimental results of Moreyra and Peköz(1994a) are compared in Table 1 with the AISI predictions and ABAQUS results using the six foot beam model described in this section. Tests "B-TB" and "C-TB" are the same as test "A-TB" except the lip sizes were 1" (25.4 mm) and 7/8" (22.23 mm), respectively. Clearly, ABAQUS is more accurate in its predictions. Test C-TB had its compression lip sheared. The effects of shearing on the material properties may be the reason for its lack of correlation to predicted strengths [see Moreyra and Peköz(1994a) on the effects of shearing the lip].

3. RESULTS OF THE PARAMETRIC STUDIES

The results of the parametric studies using the six foot beam finite element model described in the previous section, are summarized in Table 2.

A parametric study that varies C-section element sizes allows for a greater understanding of the relationships that exist amongst the elements. The parametric study described in this report contains three variables: lip length, flange width, and web height. Table 3 lists the section names and element sizes associated with each name. The name designation scheme in the table is fairly simple. The first set of characters defines the web height: sections H1, H2, and H3 have web heights of 6", 8", and 10" respectively. The second set of characters in the name describe the flange width: sections W0, W1, W2, and W3 have flange widths of 1.625", 2.5", 3.5", and 4.5", respectively. The last number in the section name is the lip length, D, defined in Fig. 1.

3.1 Ultimate Moment

The ABAQUS ultimate moment is compared with the nominal moment capacity predicted by the 1986 AISI Specification in Table 2. The ABAQUS moment is assumed to be a "test" moment so that the adequacy of the Specification can be determined by examining the ratio M_t/M_n. M_t is the ABAQUS failure moment and M_n is the moment capacity calculated according to AISI SPecification (1991). The average (AVG) and coefficient of variation (COV) of this ratio is calculated for each web height in Table 2. The average and COV of all the finite element analyses combined are 0.805 and 0.0853, respectively.

Moment versus the lip length for both the ABAQUS results and AISI predictions are plotted in Fig. 5. This allows one to see the effect of lip length on section strength. The objective of Figs. 6 through 9 is to locate the origin of these unconservative results in the AISI Specification. This is done by plotting M_t/M_n versus several element sizes and element ratios. Only a few sets of parametric study sections are plotted since the other sets follow the same trends.

The results that are evident in the tables and the figures are:

- The correlation between ABAQUS and AISI decreases as web height increases. This is obvious by the decreasing average and COV values of M_t/M_n ratios as web height increases.
- The ABAQUS results are significantly lower than the AISI predictions of ultimate moment.
- The ABAQUS moment versus lip length curve approaches zero slope as the lip length increases. This implies that an optimum lip length is reached by the section beyond which there is no further increase in strength. Although not shown, this is true for all web-flange combinations.
- The AISI Specification assumes the section strength to decrease beyond a limiting D/w ratio. This is not evident in any of the ABAQUS results.
- The M_t/M_n ratio decreases significantly as the flange width increases. This suggests that improvements in the flange effective width equations are necessary.
- Narrow flanges are more affected by the web than wide flanges. This is demonstrated by a significant change in the strength of narrow flanged sections as web height increases.
- When the flange is wide, web support is inconsequential. This is most likely due to the fact that the flange goes into a post-buckling range at a very low load level.

3.2 Failure Modes

At failure, buckling waves were clearly visible in the three-dimensional finite element model. These waves were dominant in one of three modes: local web, local flange, and distortional. The ABAQUS deformed shape for these three modes is shown in Figs. 10, 11, and 12. Note that the deformed shape displacements in these figures are magnified seven times. The failure mode for each finite element model is listed in Table 2 and results are compared to those obtained by an elastic buckling analysis program called BFINST.

BFINST [Hancock(1978)] is based on the finite strip method. Critical elastic buckling stress for the section, the critical buckling mode, and the buckling wavelengths for each mode can be obtained from BFINST. Table 2 clearly shows that the ABAQUS results agree very well with the BFINST results in every case except the H3-W2 sections.

A few clear patterns emerge when one compares the failure modes to the element stress distributions at failure:

- When the distortional mode prevails, the web always has linear stress distribution. If local web buckling failure occurs, the stress distribution in the web is non-linear.
- Sections which buckle in the distortional mode correlate the least with the AISI ultimate moment predictions.

3.3 Stresses

The stresses discussed in this Section are at the maximum stress location along the beam. In all cases, the highest stresses occurred at a point where an initial imperfection was placed. It is important to note that the maximum stress for the web and flange may have occurred at different span locations.

At failure, the stresses along the flange were distributed in one of four ways as drawn in Fig. 13. The stresses examined are for the flat width portion of the flange. Distribution shapes F4 and F1 are similar to the theoretical stress distributions for stiffened and unstiffened elements, respectively.

The compression flange stresses observed at the ultimate load are tabulated in Table 2. This table also lists the ratio of edge stresses, F_a/F_b where F_a is the minimum and F_b is the maximum edge stress in the flange (see Fig. 13), which may be helpful in determining or defining an "adequate" lip size. An example of flange stress distribution and edge stress ratio versus lip size is shown in Fig. 14 for H2-W2 sections.

Typical web stress distributions obtained from ABAQUS are shown in Fig. 15. It may be assumed that webs with a stress pattern equal to W1 are fully effective while those with pattern W2 are not. Effect of lip size on web stresses for H3-W2 sections is shown in Fig. 16. Maximum web stresses for all other members are tabulated in Table 2.

The compression lip stress distributions are typically the same for all parametric study sections. These stresses are almost always in compression at failure. There are a few exceptions: for example, a section with a "long lip" (approximately 1.3" or 1.4") may exhibit slight (5 to 10 ksi) tensile stresses at the tip.

4. CONCLUSIONS

The results presented in this paper lead to the conclusions listed below:

- AISI over-predicts the bending capacity of C-sections in bending when compared to ABAQUS tests.
- The web element size affects the flange element behavior.
- An optimum lip size is reached beyond which no further increase in load is obtained. AISI assumes that beyond a certain lip length, the section strength decreases. ABAQUS findings does not lead to such a conclusion.
- The correlations between AISI and ABAQUS become increasingly worse as flange width increases. Therefore, modifications in the flange effective width formulations may be necessary.
- A problem with the web effective width equations may exist since the AISI correlations decrease as web height increases.
- The stresses in most sections do not reach yield.
- All sections that undergo local web buckling at failure have W2 (non-linear) web stress distributions. This may imply that all sections which undergo local web buckling at failure have webs that are not fully effective.

5. ACKNOWLEDGEMENTS

This paper is based on a thesis presented to the Graduate School of Cornell University for the degree of Master of Science by Maria E. Moreyra. This work was sponsored at Cornell University by the American Iron and Steel Institute. The valuable support and contributions of the members of the AISI Subcommittee on Element Behavior and its Chairman Mr. D. L. Johnson are gratefully acknowledged.

APPENDIX - REFERENCES

ABAQUS (1989). Users Manual Version 4.8. Hibbit, Karlsson and Sorensen, Inc.

American Iron and Steel Institute (1991), " Load and Resistance Factor Design Specification for Cold-Formed Steel Structural Members, March 16, 1991 Edition

Hancock, G. J.(1978), "BFINST6: An Elastic Finite Strip Buckling Analysis Program," University of Sydney, Australia, 1978

Moreyra, M. E. and Peköz, T. (1994a), "Experiments on Lipped Channel Flexural Members," Proceedings of the Twelfth International Specialty Conference on Cold-Formed Steel Structures, University of Missouri-Rolla, October 1994

Moreyra, M. E. and Peköz, T. (1994b), "A Design Procedure for Lipped Channel Flexural Members," Proceedings of the Twelfth International Specialty Conference on Cold-Formed Steel Structures, University of Missouri-Rolla, October 1994

Moreyra, M. E. and Peköz, T. (Project Director) (1993), "Behavior of Cold-Formed Steel Lipped Channels under Bending and Design of Edge Stiffened Elements," Research Report 93-4, School of Civil and Environmental Engineering, Cornell University, June 1993

Willis, C. T. and Wallace, B. J.(1990a), "Behavior of Cold-Formed Steel Purlins Under Gravity Loading," Journal of Structural Engineering, Vol. 116, No. 8, August 1990, 2061-2069

Willis, C. T. and Wallace, B. J.(1990b), "Wide Lips - A Problem With the AISI Code," Proceeding of the Tenth International Specialty Conference on Cold-Formed Steel Structures, St. Louis, MO, October 23-24

APPENDIX - NOTATION

D, H, h, R, T, W, w Cross-sectional dimensions defined in Fig. 1
F_a Edge stress (see Fig. 13)
F_b Edge stress (see Fig. 13)
M_{ABAQ} Nominal moment capacity calculated by ABAQUS (1989)
M_n Nominal moment capacity calculated according to the AISI Specification (1991)
M_{test} Nominal moment capacity calculated by ABAQUS (1989)
P Defined in Section 2.8

Table 1 "TB" experiment results compared to AISI predictions, and ABAQUS results.

Experiment Name	Mn^1 (k-in)	M_{ABAQ} (k-in)	M_{test} (k-in)
A-TB	159.3*	130.9	127.4
B-TB	150.1*	121.7	123.9
C-TB	146.6*	120.8	132.6

notes:
1 Mn is calculated using the AISI Specification
* Web is fully effective

Table 2 Parametric Study Results

TEST	H	W	D	w	h	M_t	$\frac{M_t}{M_n}$	(1)	(2)	(3)	(4)	(5)	(6)	(7)	(8)
H1-W0-0.6	6	1.63	0.60	1.11	5.48	44.0	0.885	D	D	W1	39	0.78	F1	0.81	1.00
H1-W0-0.8	6	1.63	0.85	1.11	5.48	46.2	0.883	D	D	W1	38	0.76	F1	0.79	1.00
H1-W0-1.1	6	1.63	1.10	1.11	5.48	47.9	0.905	D	D	W1	38	0.76	F1	0.79	1.00
H1-W1-0.3	6	2.50	0.35	1.98	5.48	39.2	0.808	D	D	W1	27	0.54	F2	0.74	0.80
H1-W1-0.6	6	2.50	0.60	1.98	5.48	48.7	0.877	D	D	W1	29	0.58	F2	0.72	0.92
H1-W1-0.8	6	2.50	0.85	1.98	5.48	54.7	0.887	D	D	W1	32	0.64	F2	0.75	0.98
H1-W1-1.1	6	2.50	1.10	1.98	5.48	59.3	0.927	D/LFD		W1	35	0.70	F2	0.79	0.98
H1-W1-1.2	6	2.50	1.20	1.98	5.48	60.5	0.956	LF	LF	W1	42	0.84	NA	NA	NA
H1-W1-1.3	6	2.50	1.30	1.98	5.48	61.7	0.987	LF	LF	W1	42	0.84	NA	NA	NA
H1-W1-1.4	6	2.50	1.40	1.98	5.48	62.5	1.016	LF	LF	W1	42	0.84	NA	NA	NA
H1-W2-0.6	6	3.50	0.60	2.98	5.48	47.2	0.793	D	D	W1	25	0.50	F4	0.70	0.84
H1-W2-0.8	6	3.50	0.85	2.98	5.48	55.7	0.834	LF	D	W1	30	0.60	F4	0.82	0.82
H1-W2-1.0	6	3.50	1.00	2.98	5.48	57.4	0.803	LF	LF	W1	33	0.66	F4	0.85	0.86
H1-W2-1.1	6	3.50	1.10	2.98	5.48	59.5	0.816	LF	LF	W1	33	0.66	F4	0.88	0.84
H1-W2-1.2	6	3.50	1.20	2.98	5.48	59.5	0.821	LF	LF	W1	31	0.62	F4	0.88	0.90
H1-W3-0.6	6	4.50	0.60	3.98	5.48	42.4	0.689	D/LFD		W1	22	0.44	F3	0.75	0.64
H1-W3-0.8	6	4.50	0.85	3.98	5.48	50.4	0.728	LF	LF	W1	27	0.54	F4	0.78	0.96
H1-W3-1.0	6	4.50	1.00	3.98	5.48	53.3	0.716	LF	LF	W1	26	0.52	F4	0.71	1.02
H1-W3-1.1	6	4.50	1.10	3.98	5.48	55.5	0.714	LF	LF	W1	26	0.52	F4	0.71	1.02
H1-W3-1.2	6	4.50	1.20	3.98	5.48	56.5	0.721	LF	LF	W2	27	0.54	F4	0.77	0.94
H1-W3-1.3	6	4.50	1.30	3.98	5.48	58.1	0.745	LF	LF	W2	29	0.58	F4	0.84	0.86
MEAN							0.834								
C.O.V.							0.111								

Notes:
(1) Failure modes according to ABAQUS. D = Distortional, LW = Local Web, LF = Local Flange (See Figs. 11, 12, 13 for 3-D sketches)
(2) Failure mode according to BINST [Hancock (1973)]
(3) Web stress distribution type (see Fig. 15)
(4) Maximum stress in web
(5) Maximum stress in web / Yield stress
(6) Flange stress distribution type (see Fig. 13)
(7) F_a / F_b (see Fig. 13)
(8) Maximum stress in flange / Yield stress
M_t Moment capacity calculated by ABAQUS (1989), k-in (1 k-in = 113 N-m)

Table 2 Parametric Study Results (Cont.)

TEST	H	W	D	w	h	M_t	$\frac{M_t}{M_a}$	(1)	(2)	(3)	(4)	(5)	(6)	(7)	(8)
H1-W0-0.6	8	1.63	0.60	1.11	7.48	60.5	0.805	LW	LW	W2	46	0.92	F1	0.68	0.82
H1-W0-0.8	8	1.63	0.85	1.11	7.48	63.4	0.801	LW	LW	W2	49	0.98	F1	0.40	0.86
H1-W0-1.1	8	1.63	1.10	1.11	7.48	65.2	0.812	LW	LW	W2	50	1.00	F1	0.34	0.88
H1-W1-0.3	8	2.50	0.35	1.98	7.48	56.7	0.785	D	D	W1	30	0.60	F1	0.79	0.82
H1-W1-0.6	8	2.50	0.60	1.98	7.48	67.0	0.807	LW	D	W1	40	0.80	F1	0.04	0.78
H1-W1-0.8	8	2.50	0.85	1.98	7.48	75.1	0.820	LW	LW	W2	50	1.00	F1	0.06	0.84
H1-W1-1.1	8	2.50	1.10	1.98	7.48	80.3	0.843	LW	LW	W2	50	1.00	F2	0.41	0.70
H1-W1-1.2	8	2.50	1.20	1.98	7.48	81.0	0.856	LW	LW	W2	55	1.10	F3	0.37	0.70
H1-W1-1.3	8	2.50	1.30	1.98	7.48	80.5	0.860	LW	LW	W2	50	1.00	F3/F4	0.63	0.62
H1-W1-1.4	8	2.50	1.40	1.98	7.48	51.5	0.882	LW	LW	W2	56	1.12	F3/F4	0.72	0.62
H1-W2-0.6	8	3.50	0.60	2.98	7.48	65.3	0.769	D	D	W1	27	0.54	F4	0.74	0.88
H1-W2-0.8	8	3.50	0.85	2.98	7.48	77.7	0.803	LF	D	W1	32	0.64	F4	0.83	0.88
H1-W2-1.1	8	3.50	1.10	2.98	7.48	83.3	0.776	LF	LF	W1	36	0.72	F4	0.92	0.88
H1-W2-1.2	8	3.50	1.20	2.98	7.48	84.7	0.795	LF	LF	W1	42	0.84	F4	0.93	0.90
H1-W2-1.3	8	3.50	1.30	2.98	7.48	86.1	0.816	LF	LF	W2	38	0.76	F4	0.93	0.82
H1-W2-1.4	8	3.50	1.40	2.98	7.48	86.5	0.829	LF	LF	W2	36	0.72	F4	0.94	0.76
H1-W3-0.6	8	4.50	0.60	3.98	7.48	58.6	0.697	D	D	W1	23	0.46	F4	0.75	0.68
H1-W3-0.8	8	4.50	0.85	3.98	7.48	71.1	0.738	LF	D	W1	31	0.62	F4	0.81	1.00
H1-W3-1.0	8	4.50	1.00	3.98	7.48	77.8	0.741	LF	LF	W2	31	0.62	F4	0.82	0.94
H1-W3-1.1	8	4.50	1.10	3.98	7.48	79.0	0.714	LF	LF	W2	29	0.58	F4	0.78	0.92
H1-W3-1.2	8	4.50	1.20	3.98	7.48	80.1	0.716	LF	LF	W2	30	0.60	F4	0.85	0.94
MEAN							0.793								
C.O.V.							0.062								

TEST	H	W	D	w	h	M_t	$\frac{M_t}{M_a}$	(1)	(2)	(3)	(4)	(5)	(6)	(7)	(8)
H1-W0-0.6	10	1.63	0.60	1.11	9.48	73.5	0.744	LW	LW	W2	50	1.00	F1	0.20	0.96
H1-W0-0.8	10	1.63	0.85	1.11	9.48	79.7	0.764	LW	LW	W2	55	1.10	F1	0.10	0.96
H1-W0-1.1	10	1.63	1.10	1.11	9.48	82.5	0.786	LW	LW	W2	55	1.10	F1	0.11	0.86
H1-W1-0.3	10	2.50	0.35	1.98	9.48	73.5	0.824	D	D	W1	43	0.86	F1	0.24	0.66
H1-W1-0.6	10	2.50	0.60	1.98	9.48	82.8	0.802	D	LW	W1	42	0.84	F1	0.21	0.82
H1-W1-0.8	10	2.50	0.85	1.98	9.48	92.8	0.799	D/LW	LW	W2	50	1.00	F1	0.13	0.92
H1-W1-1.1	10	2.50	1.10	1.98	9.48	99.8	0.819	LW	LW	W2	55	1.10	F2	0.32	0.74
H1-W1-1.2	10	2.50	1.20	1.98	9.48	101.3	0.842	LW	LW	W2	50	1.00	F3	0.58	0.66
H1-W1-1.3	10	2.50	1.30	1.98	9.48	101.5	0.857	LW	LW	W2	55	1.10	F3	0.56	0.66
H1-W1-1.4	10	2.50	1.40	1.98	9.48	101.3	0.872	LW	LW	W2	52	1.04	F3	0.60	0.66
H1-W2-0.6	10	3.50	0.60	2.98	9.48	83.9	0.795	D	D	W1	28	0.56	F4	0.79	0.78
H1-W2-0.8	10	3.50	0.85	2.98	9.48	99.6	0.827	LF	LW	W2	33	0.66	F4	0.84	0.88
H1-W2-0.9	10	3.50	0.95	2.98	9.48	101.8	0.823	LF	LW	W2	33	0.66	F4	0.85	0.84
H1-W2-0.9	10	3.50	1.10	2.98	9.48	103.6	0.815	LF	LW	W2	33	0.66	F4	0.88	0.84
H1-W2-1.0	10	3.50	1.20	2.98	9.48	104.4	0.798	LF	LW	W2	32	0.64	F4	0.88	0.80
H1-W2-1.1	10	3.50	1.30	2.98	9.48	105.6	0.787	LF	LW	W2	33	0.66	F4	0.92	0.74
H1-W3-0.6	10	4.50	0.60	3.98	9.48	75.5	0.716	D	D	W1	24	0.48	F4	0.74	0.74
H1-W3-0.8	10	4.50	0.85	3.98	9.48	93.0	0.771	LF	D	W1	34	0.68	F4	0.84	0.96
H1-W3-0.9	10	4.50	0.95	3.98	9.48	96.4	0.755	LF	LF	W1	34	0.68	F4	0.84	1.02
H1-W3-1.0	10	4.50	1.00	3.98	9.48	97.8	0.744	LF	LF	W2	34	0.68	F4	0.88	0.94
H1-W3-1.1	10	4.50	1.10	3.98	9.48	95.1	0.685	LF	LF	W2	30	0.60	F4	0.98	0.64
H1-W3-1.2	10	4.50	1.20	3.98	9.48	102.6	0.731	LF	LF	W2	31	0.62	F4	0.96	0.76
MEAN.							0.789								
C.O.V.							0.058								

Notes: See preceeding page for notes (1) through (8).

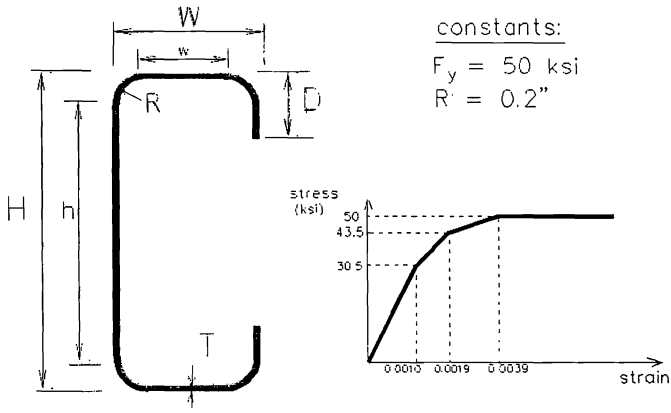

Fig. 1 Parametric study variables and constants.

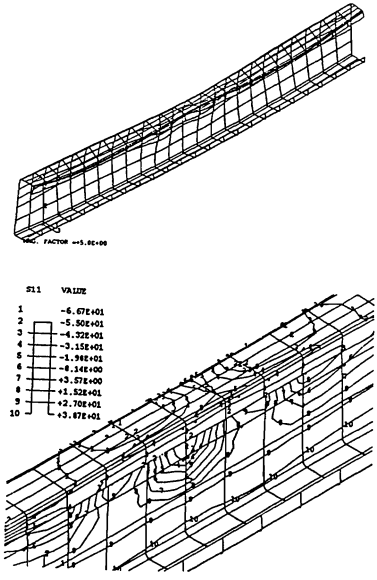

Fig. 2 Deformed mesh and contour lines of stresses in the x-direction at failure. Contour lines of stresses are shown at mid-span.

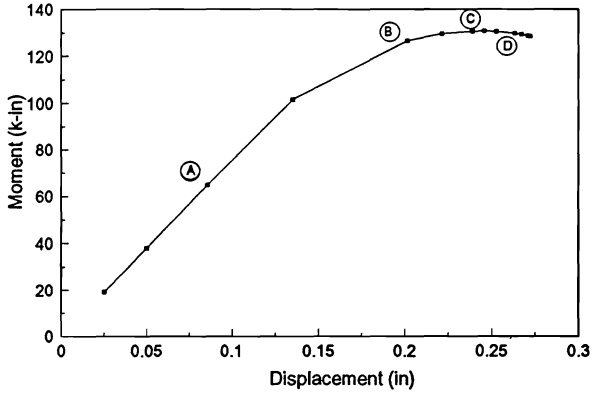

Fig. 3 Moment versus maximum vertical displacement curve of chosen model.

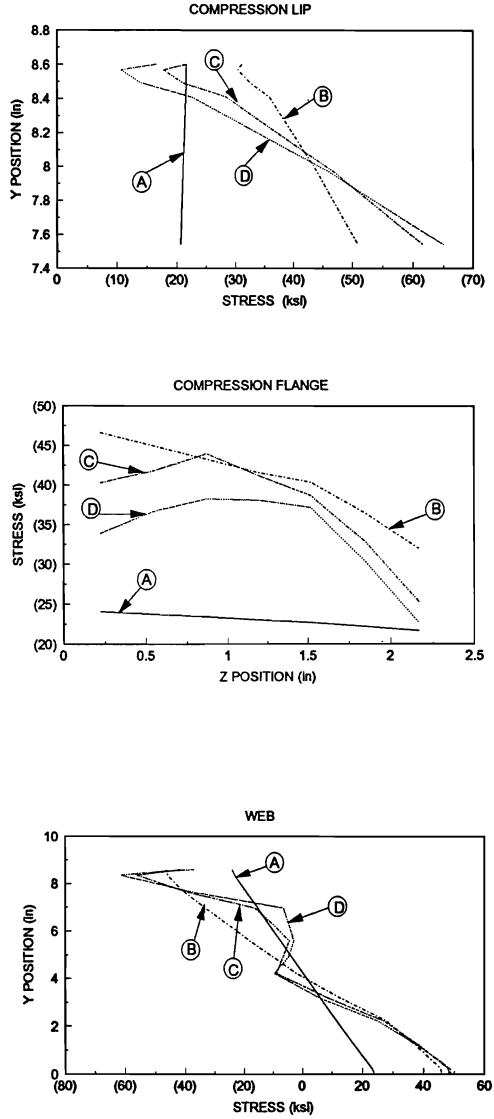

Fig. 4 Midspan stresses of the control test model (see Fig. 3)

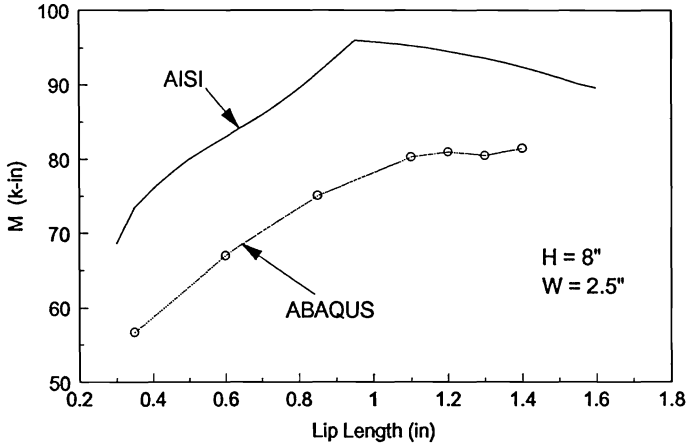

Fig. 5 ABAQUS moment and AISI moment versus lip length for H2-W1 sections.

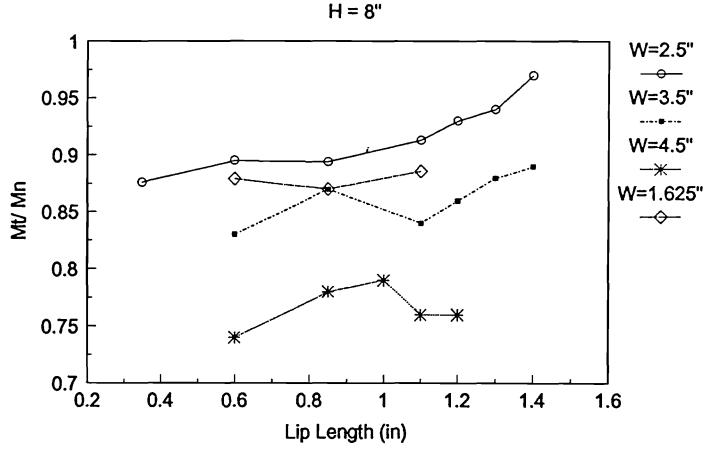

Fig. 6 Mt / Mn versus lip length for all flange sizes and a web height of 8". (Mt = ABAQUS; Mn = AISI).

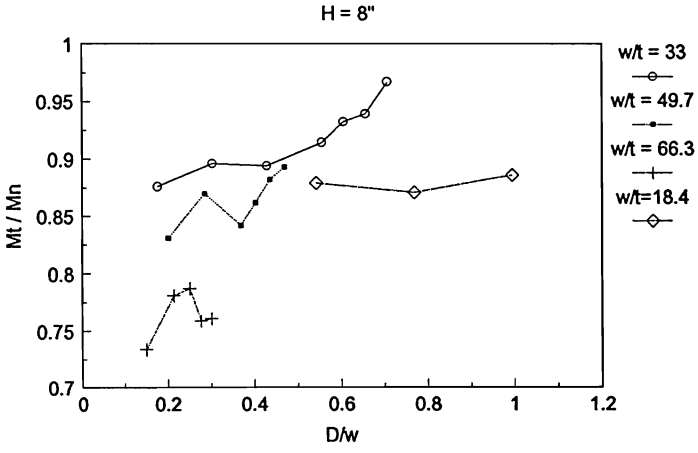

Fig. 7 M_t/M_n versus D/w for various flange slenderness ratios and a web height of 8". (Mt = ABAQUS; Mn = AISI).

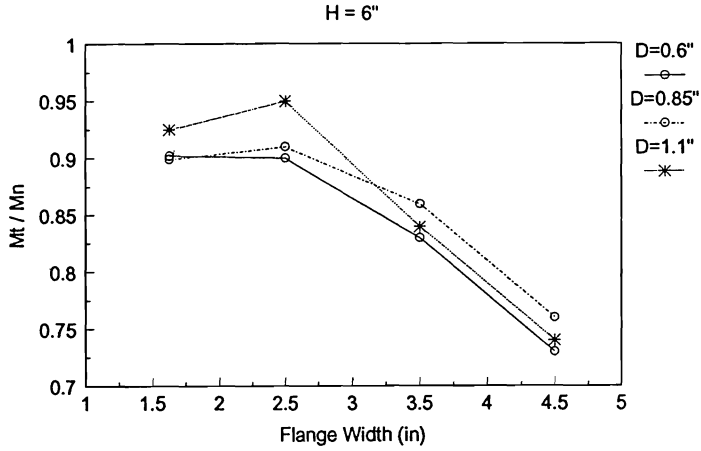

Fig. 8 Mt / Mn versus flange width, W, for several lip sizes and a web height of 8". (Mt = ABAQUS; Mn = AISI).

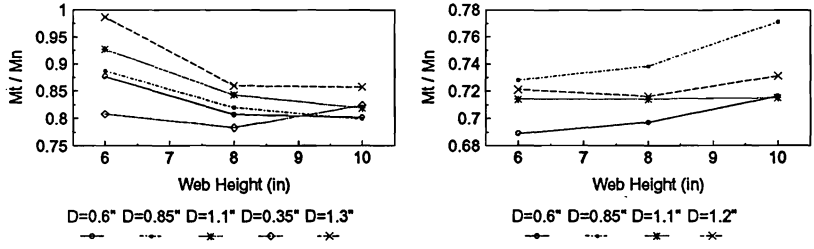

(a) Flange width W = 2.5" (b) Flange width W = 4.5"

Fig. 9 Mt / Mn versus web height for several lip lengths. (Mt = ABAQUS; Mn = AISI)

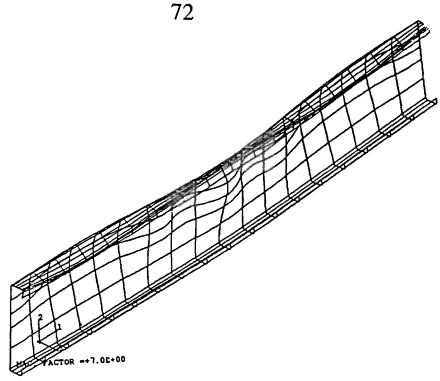

Fig. 10 ABAQUS deformed shape for the local web buckling mode. Section H3-W0-0.85.

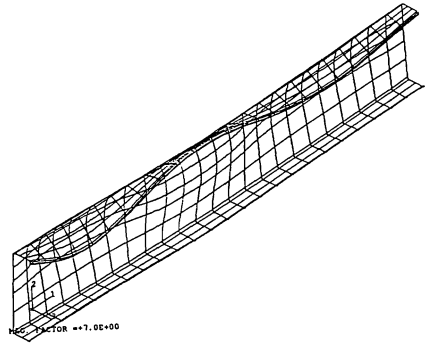

Fig. 11 ABAQUS deformed shape for the distortional buckling mode. Section H3-W1-0.35.

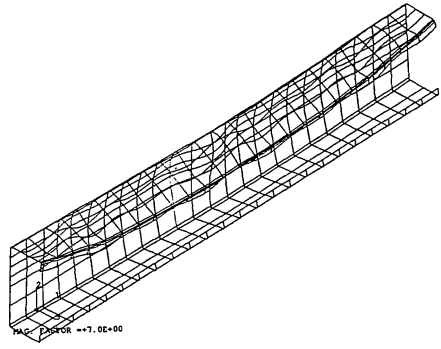

Fig. 12 ABAQUS deformed shape for the local flange buckling mode. Section H3-W3-1.0.

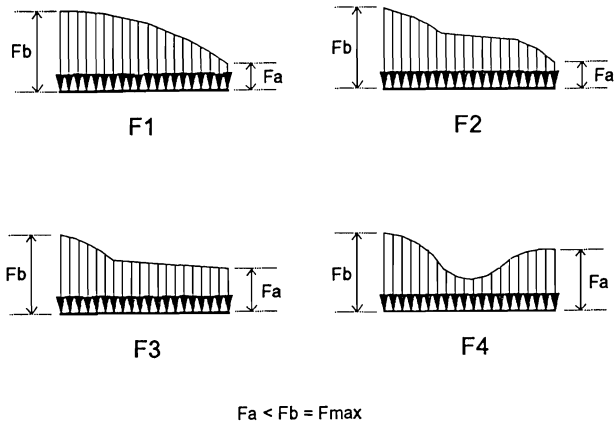

Fig. 13 Flange stress distributions

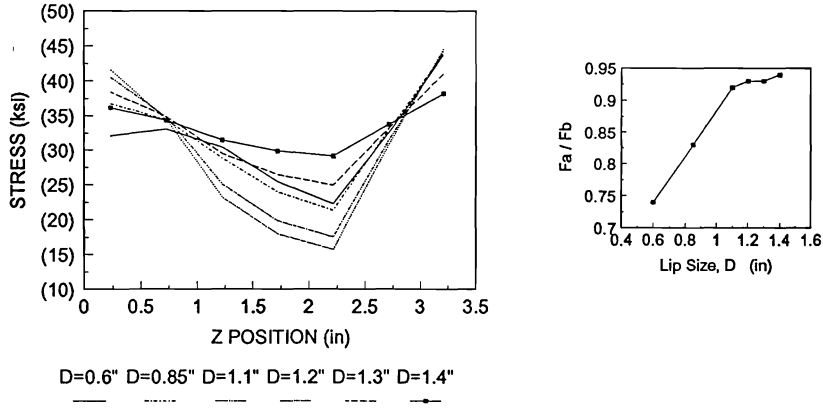

Fig. 14 Lip length effect on compression flange stresses for sections H2-W2.

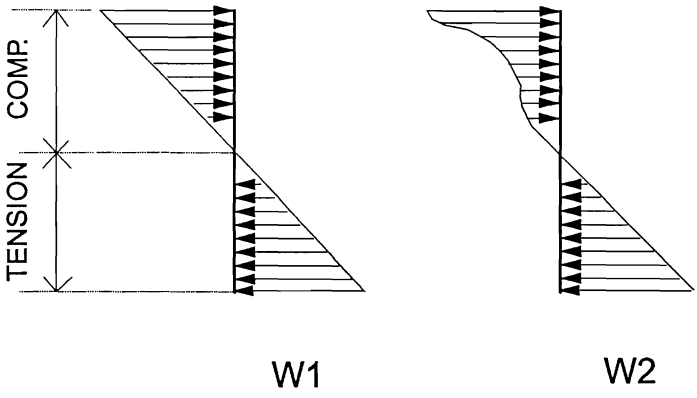

Fig. 15 Web stress distributions. (Reference for Table 6)

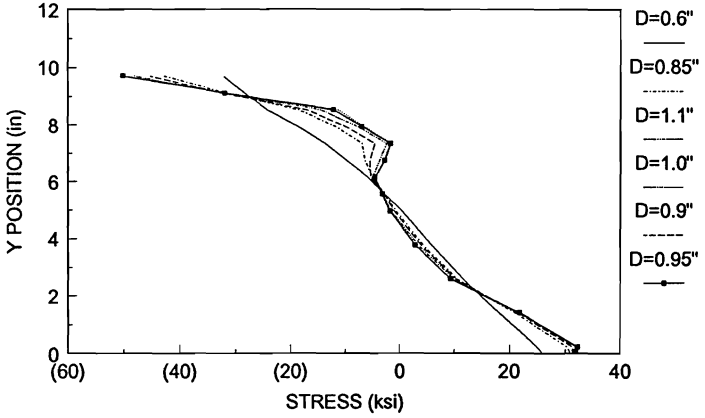

Fig. 16 Lip length effect on web stresses for sections H3-W2.